Spin transitions in a small Si quantum dot

L. P. Rokhinson, L. J. Guo,* S. Y. Chou, and D. C. Tsui

Department of Electrical Engineering, Princeton University, Princeton, New Jersey 08544
(Received 15 May 2000; published 2 January 2001)

We investigated electron transport through an ultrasmall Si quantum dot. The B dependence of energy levels is dominated by the Zeeman shift, allowing us to measure the spin difference between two successive ground states directly. Combined with the ability to change the number of electrons N in the dot between 0 and 30, we are able to map the spin of the dot as a function of N and B. The dot becomes spontaneously polarized at $N=6$ with a large spin change $\Delta S=3/2$, demonstrating the essential features of spin blockade. Surprisingly, for $N>20$, the transitions with $\Delta S>1/2$ do not lead to the suppression of the corresponding peaks at low temperatures.

The spin configuration of quantum dots is a very attractive and challenging theoretical problem, but it proved to be a formidable task to measure the spin of a few electron mesoscopic system experimentally.[1] Several experiments addressed spin-related phenomena in quantum dots directly, by either studying the Kondo effect,[2] the Zeeman shift of energy levels[3] or by injecting spin-polarized electrons into the dot.[4] So far, the most successful mapping of spins in a few electron dot has been achieved indirectly, by comparing an experimentally obtained addition spectrum to the theoretically calculated energy spectrum for a particular geometry.[5,6] In the most versatile and well studied vertical and lateral quantum dots, where electrons are weakly confined by electrostatic gates, the magnetic field B dependence of their energy levels is dominated by orbital effects, and both the addition spectrum and its B dependence can be calculated for a few simple geometries. Using this method, a spectacular zero-field polarization of circular dots, similar to the Hund's rule in atomic physics, has been deduced.[6] The nonzero spin polarization was found to build up incrementally in $\Delta S=1/2$ steps, as electrons were added into the dot. No direct evidence of transitions involving a large spin change $\Delta S>1/2$ has yet been reported.

In this paper we report direct measurements of the spin in a few-electron quantum dot. We use a small Si quantum dot, which uniquely combines the flexibility to change the number of electrons N in the dot from 0 to 30 with the strong electron confinement provided by the sharp Si/SiO$_2$ interface. At $B<13$ T, the B dependence of energy levels is dominated by the Zeeman shift and we are able to measure the difference between the spin of the successive ground states $\Delta S=S(N)-S(N-1)$ directly as electrons are added into the dot one by one. The first five electrons are added in a spin-up–spin-down sequence at $B=0$, and we are able to follow the evolution of $S(N)$ through the singlet- triplet-spin-polarized configurations as a function of B. The ground state with $N=6$ has $S>1/2$ even at $B=0$. Remarkably, the polarization is not achieved incrementally in $\Delta S=1/2$ steps, but, rather, by the change of the total spin by $\Delta S=3/2$. Such transitions were theoretically suggested as a possible mechanism for the suppression of some Coulomb blockade (CB) peaks at low temperatures, the so-called spin blockade.[7] Indeed, the 6th peak is strongly suppressed at low temperatures

in the range of B, where $\Delta S=3/2$. For larger numbers of electrons, $N>20$, we observed transitions with $\Delta S=3/2$ with no apparent suppression of the peaks at low T. The spin scattering mechanism involved is not currently understood.

The measurements were performed on a small Si quantum dot fabricated from a silicon-on-insulator wafer. The dot resides inside a narrow bridge patterned from the top Si layer (see inset in Fig. 1). A 50 nm thick layer of thermal oxide is grown around the bridge followed by a poly-Si gate. The fabrication steps have been described previously in details.[8] Gate capacitance is estimated to be 0.8–1.0 aF, consistent with 150–200 mV peak spacing, the total capacitance C ≈ 15 aF and the charging energy $U_c=e/C\approx 10$ meV. Spacing between excited levels $\delta\sim 1-4$ meV, measured using nonzero bias spectroscopy, is comparable to the charging energy and is consistent with the lithographical size of the dot $l\approx\sqrt{\hbar/m^*\delta}\approx 100-190$ Å. The gate voltage to en-
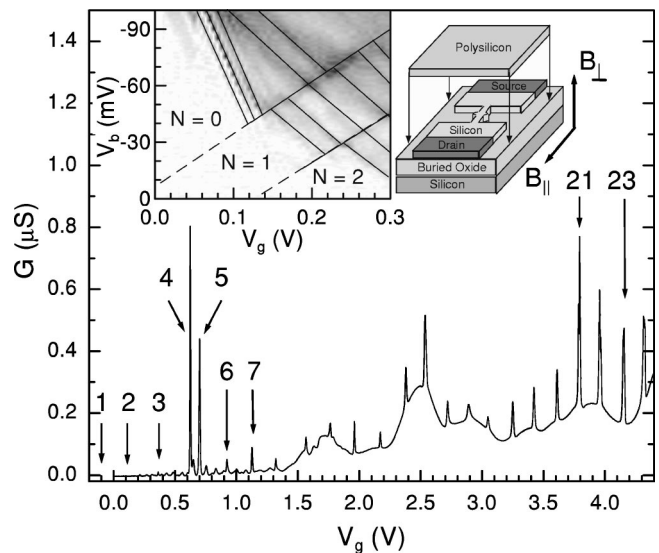

FIG. 1. Conductance as a function of gate voltage measured at $T=1.5$ K and $B=0$. Peaks are numbered in sequence starting from the entrance of the first electron into the dot (peak 1). In the left inset, differential conductance as a function of V_g and V_b is plotted, darker regions represent higher conductance. The lines highlight positions of the peaks. The right inset is a schematic of the device.

ergy conversion coefficient, measured from both nonzero bias spectroscopy and T dependent scaling of the peak width, is $\alpha \approx 14$ mV/meV.

A representative trace of the conductance G as a function of the gate voltage V_g at $T = 1.5$ K is shown in Fig. 1. Commonly for this type of devices, the sample has a parallel conducting channel,[9] which can be seen as a nonmonotonic background at $V_g > 1.5$ V; the parallel conduction is suppressed at 60 mK. Electrical transport through the dot and the parallel channel are decoupled, because Coulomb blockade peaks remain thermally broadened within the whole range of V_g studied. For further discussion, it is important to determine the exact number of electrons in the dot. At zero bias, the lowest peak is observed at $V_g = 0.34$ V. A high-T threshold voltage is -0.2 V and there may be 2–3 more peaks that are not resolved. Indeed, from high-bias spectroscopy we can determine positions of two more peaks at -0.02 and 0.12 V (see inset in Fig. 1). There is a distinct feature in the spectrum that allows us to determine the entrance of the first electron unambiguously. When the dot has a finite number of electrons, the dot potential is determined by the ratio of the source C_s, drain C_d, and gate C_g capacitances, in particular, the exited levels and the boundaries of the CB regions have a slope $dV_b/dV_g = -C_g/C_d \approx -0.2$ for $V_g < 0.3$ V (this ratio decreases to -0.11 for $V_g > 0.5$ V). However, the lowest V_g boundary has a much larger slope of $dV_b/dV_g \approx -1.0$. This large slope boundary marks the entrance of the first electron, because for the empty dot there are no corresponding C_d and C_g, and the dot potential is approximately an arithmetic average between V_g and V_b.

The peak position as a function of V_g is determined by the degeneracy condition that the electrochemical potentials for the ground states with $N-1$ and N electrons in the dot are equal. It has long been realized[10] that for noninteracting electrons the field dependence of the peak positions $V_g^p(B)$ can be directly mapped onto the single-particle energy spectrum of the dot $E(N,B)$, provided that the Fermi energy E_F in the contacts is field independent. For $V_g < 0.4$ V (the first three peaks), the electron density in the contacts is low and the contacts are spin polarized in a moderate magnetic field. For $V_g > 0.4$ V ($N \geq 4$) both spin subbands are occupied within the experimental range of $0 < B < 13$ T, the E_F becomes field independent and the peak shift reflects only the field dependence of the energy levels in the dot (also, mobility of the two-dimensional gas is low, ≈ 300 cm^2/V s at 4.2 K, and there is no measurable modulation of E_F due to Subnikov–de Haas oscillations for B up to 13 T).

The change in peak position as a function B is plotted in Fig. 2 for peaks 4–32. The measurements were repeated for two different orientations of B, defined in the inset in Fig. 1. We found that V_g^p is insensitive to the direction of B: aligning B with the current direction ($B_\parallel$, in plane) or perpendicular to the plane of the sample ($B_\perp$) does not change V_g^p significantly. Our lithographically defined dot is elongated along the bridge axis and orbital effects are expected to depend on the direction of B. Thus, we conclude that in our small dot the B dependence of V_g^p is dominated by spin effects. This conclusion is also supported by the observation that, in the
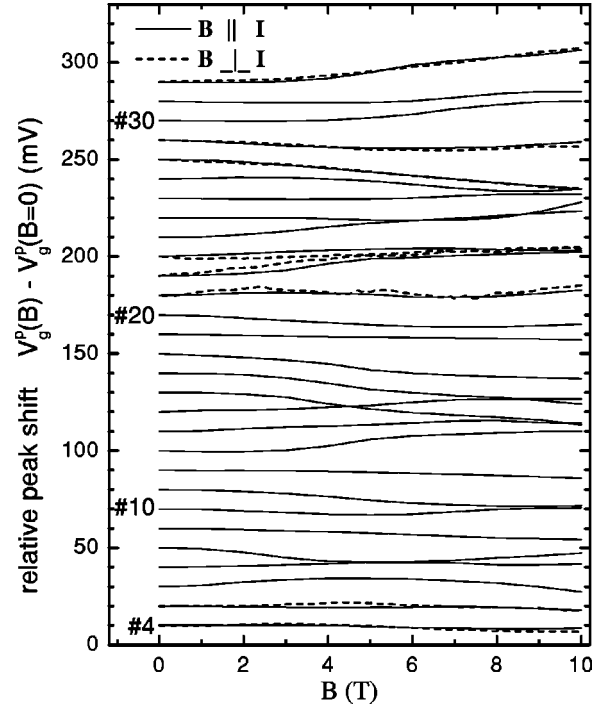

FIG. 2. Relative shift of peaks $V_g^p(B) - V_g^p(0)$ is plotted as a function of B for peaks 4–32. Each curve is offset by 10 mV (≈ 0.7 meV). Solid lines are for $B \| I$ (in plane) and dashed lines are for $B \perp I$ (normal to the sample surface). Data were taken at 1.5 K, except for the peaks 21, 22 and 23 at $B \perp I$, which were taken at 60 mK in a different cooldown.

range of B when the contacts are fully spin polarized, the V_g^p for peaks 1–3 does not depend on B at all.

Unlike V_g^p, the peak amplitude G^p depends on the direction of B. The G^p reflects the tunneling probability and depends exponentially on the overlap of wave functions in the dot and in the contacts. As such, G^p is sensitive to the particular configuration of the wave function within the dot, and any redistribution of the wave function due to small orbital effects can result in a significant change of G^p.

For a quantitative analysis, peak positions are extracted from G vs V_g scans, and the peak shift, $\Delta U^p(B) = [V_g^p(B) - V_g^p(0)]/\alpha$, is plotted as a function of B in Figs. 3(b) and 4(b). The curves are offset for clarity. For comparison, lines with slopes $\pm 1/2 g^* \mu_B$ for $g^* = 2$ are also shown (solid lines). First, let us focus on the low-field ($B < 2$ T) region. Peaks 4 and 5 shift linearly with B and the corresponding slopes are $+$ and $-1/2 g^* \mu_B$. In the same low-field region, the preceding peaks 2 and 3 also shift with $+$ and $-1/2 g^* \mu_B$ slopes. Thus, at low fields, the ground states with up to five electrons in the dot have the lowest spin configuration and the dot is filled in a spin-down–spin-up sequence. Such a filling sequence requires that the valley degeneracy is lifted.

This simple picture of alternating filling does not hold for $N > 5$ even at low fields. At $B < 2$ T peak 6 consists of three peaks separated by ≈ 0.5 meV at zero field, none of which shifts with $1/2 g^* \mu_B B$ [the zero-field positions of the three peaks are marked by triangles in Fig. 3(a)]. The slope of the
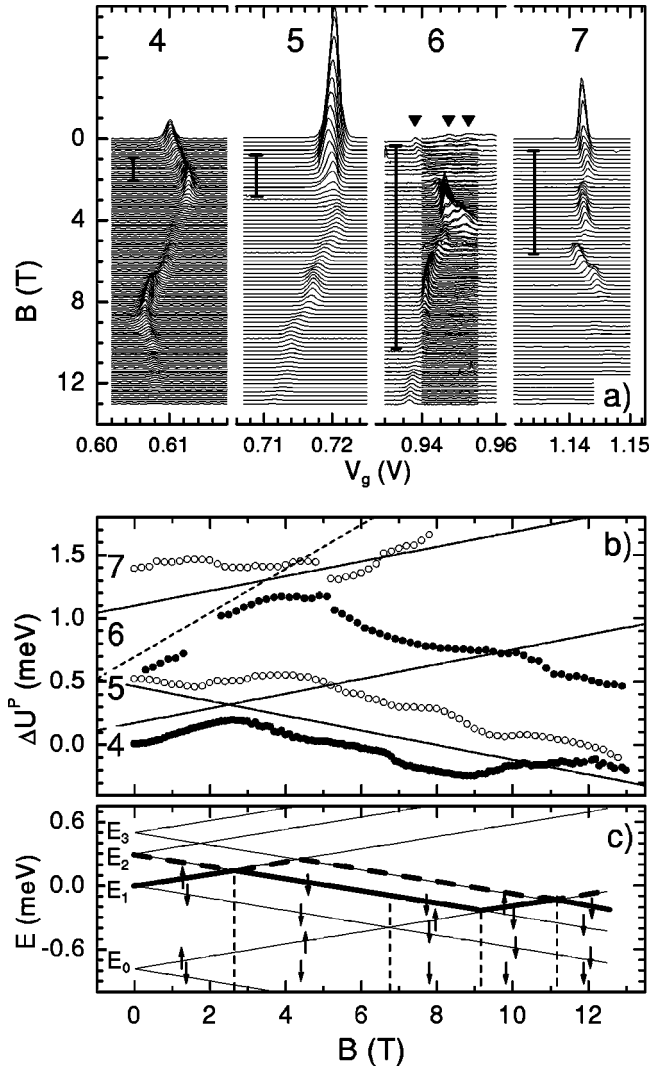
FIG. 3. (a) Conductance for four consecutive peaks was measured at 200 mK with $V_{ac} = 50$ μV. Individual traces are offset linearly with B and the vertical bars are 1 μS scales. In (b) peak shifts $\Delta U^p(B) = [V_g^p(B) - V_g^p(0)]/\alpha$ are plotted for the same four peaks. The zero-field positions are arbitrarily offset. Points are omitted if the peak conductance is <0.01 μS. Peak 6 is comprised of three peaks at $B<2$ T [marked with triangles in (a)] and only the lowest-energy branch is shown. Solid and dashed lines have slopes 1/2 and $3/2g^*\mu_B$ respectively. (c) Schematic evolution of single-particle energy levels, assuming only the Zeeman level splitting.

lowest-energy branch is close to $3/2g^*\mu_B$, the other two branches have smaller than $1/2g^*\mu_B$ negative slopes. The shift of the next, the 7th peak has a positive slope, while the lowest spin configuration for a dot with seven electrons should have a negative Zeeman shift. We conclude from these observations that the ground state with six electrons in the dot is spontaneously polarized and the total spin $S(6) > 1/2$. The transitions between the $N-1$ and N ground states that involve a change of the total spin by $\Delta S > 1/2$ have low probability and the corresponding peaks are expected to be suppressed.[7] Indeed, peak 6 is strongly suppressed at low temperatures and, presumably, the appearance of several
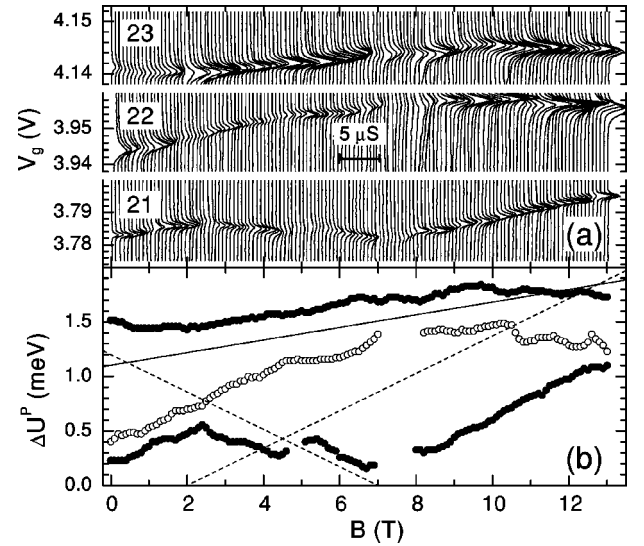

FIG. 4. (a) Evolution of peaks 21, 22, and 23 as a function of $B \perp I$. Conductance was measured at $T = 60$ mK using $V_{dc} = 20$ μV. All three data sets have the same scale. In (b) peak shifts are plotted for the same three peaks, similar to Fig. 3. Solid and dashed lines have slopes 1/2 and $3/2g^*\mu_B$, respectively.

branches can be related to the instability of the polarized state.

The low-field spin configuration is not preserved at high-magnetic fields. For peak 4, dV_g^p/dB changes sign from positive to negative at $B = 2.5$ T, back to positive at $B = 9$ T, and, again, to negative at $B \approx 12$ T. The spin of the tunneling electron changes from being $+1/2 \rightarrow -1/2 \rightarrow +1/2 \rightarrow -1/2$. The corresponding spin transitions of the ground state can be understood from a simple model for noninteracting electrons. Let us consider four single particle levels E_i, as shown in Fig. 3(c). Each level is spin degenerate at zero field and splits into two levels $E_i \pm 1/2g^*\mu_B B$ for $B > 0$. In the absence of interactions, the position of the Nth peak is determined by $U(N,B) - U(N-1,B) = \Sigma_k^N E(k,B) - \Sigma_k^{N-1} E(k,B) = E(N,B)$, where $E(k,B)$ is the energy of the kth electron, including the Zeeman contribution. $E(4,B)$ is the thick solid line in Fig. 3(c). Qualitatively, $E(4,B)$ captures the main features of V_g^p vs B for the 4th peak and the kinks can be attributed to the corresponding level crossings. The first kink at $B = 2.6$ T marks the singlet-triplet transition and the kink at 11 T corresponds to the transition from a triplet to a spin-polarized state. The singlet-triplet transition is not an exchange-driven transition, as in previously reported studies,[5,11,12] but is a result of the crossing of levels with different spins. As a result, the energy difference between the singlet and the triplet states can be continuously and controllably tuned by adjusting the magnetic field.

There are two kinks within the triplet state that do not change the total spin of the four-electron state. Below $B = 9$ T, the 4th electron tunnels into $E_2^\downarrow$ level, while above 9 T, into $E_0^\uparrow$ level, reversing its spin. At the same time the three-electron state undergoes a transition from $S(3) = 1/2$ to $3/2$, conserving the total spin of a four-electron state $S(4) = 1$. The kink at $B = 7$ T, which coincides with the crossing

of $E_0^{\uparrow}$ and $E_1^{\downarrow}$, is a small offset, which does not change the sign of dV_g^p/dB. In the absence of interactions, there should be no corresponding kink.

Spontaneous polarization of the dot for $N>6$ is beyond the description of the model of noninteracting electrons. There are some more features in our data that cannot be understood within this simple model and require many-body effects to be considered. The large number of kinks, 3–4 kinks per 10 T, requires single-particle level spacing to be ≈ 0.3 meV, smaller than the 1–4 meV measured using nonzero bias spectroscopy. Each level crossing should result in a pair of upward-downward kinks in two neighboring peaks at the same value of B. Clearly, the kinks in $V_g^p(B)$ for the pair of peaks 4 and 5 near 2 T are shifted by ≈ 0.5 T. The most notable deviation from this simple model of level crossing is shown in Fig. 4(b), where upward kinks at 2.3 T and 5.3 T in $V_g^p(B)$ for peak 21 have no corresponding downward counterparts in $V_g^p(B)$ for peak 22. Another clear inconsistency with the simple picture of level crossing can be seen in Fig. 2, where, in two instances, three neighboring peaks evolve similarly as a function of B (peaks 13, 14, 15 and 16, 17, 18). This kind of repetition is inconsistent with both level crossing and possible two- or fourfold level degeneracy in Si.

Now, we turn to the analysis of the $\Delta S>1/2$ transitions. As shown in Fig. 4(b), $\Delta U^p(B)$ for peaks 21 and 22 have linear segments with a slope $\approx 3/2g^*\mu_B B$. The shift of peak 21 has such a large slope in the whole range $0<B<13$ T, although its sign changes four times. We can rule out enhancement of the g factor because (i) there are segments in the neighboring peak 23 with the slope $1/2g^*\mu_B$ (assuming $g^*=2$), and (ii) it is known that interactions renormalize g^* at low electron densities in Si metal-oxide-semiconductor field-effect transistor (Si-MOSFET's) but g^* approaches the bulk value of two as the density increases.[13] Thus, we conclude that this large slope corresponds to a spin change $\Delta S = 3/2$. Quantum mechanical spin selection rules forbid a change of the total spin by $\Delta S>1/2$ during $N-1\leftrightarrow N$ transitions and the corresponding peaks should be suppressed (spin blockade). Such a suppression is clearly demonstrated for peak 6. However, there is no apparent suppression of peaks 21 and 22, which have the $3/2g^*\mu_B$ slopes, compared to the amplitude of peak 23, which has the regular slope of $1/2g^*\mu_B$. The absence of spin blockade requires an efficient spin scattering mechanism. The usually considered spin-orbit interaction is rather weak in Si and the scattering mechanism involved is not currently understood.

To summarize our results, we analyzed the spectrum of a few electron quantum dot. Using a device that is so small that the B dependence of its energy levels is dominated by the Zeeman energy, we were able to measure spin directly. We identify and follow the evolution of the total spin of the dot as a function of the magnetic field and the electron number. Some transitions involve the spin change $\Delta S>1/2$, which leads to the spin blockade at low T. However, we found that for some other transitions with $\Delta S>1/2$ and $N>20$ the corresponding peaks are not suppressed even at the lowest $T=60$ mK.

---

*Present address: Department of Electrical Engineering and Computer Science, University of Michigan, Ann Arbor, MI 48109.

[1] For a review on quantum dots, see *Mesoscopic Electron Transport*, Vol. 345 of *NATO Advanced Studies Institute Series E*, edited by L. P. Kouwenhoven, L. L. Sohn, and G. Schön (Kluwer, London, 1997).

[2] D. Goldhaber-Gordon, H. Shtrikman, D. Mahalu, D. Abusch-Magler, U. Meirav, and M. A. Kastner, Nature (London) **391**, 156 (1998); S. M. Cronenwett, T. H. Oosterkamp, and L. P. Kouwenhoven, Science **281**, 540 (1998); J. Schmid, J. Weis, K. Eberl, and K. v. Klitzing, Physica B **256**, 182 (1998); J. Schmid, J. Weis, K. Eberl, and K. V. Klitzing, Phys. Rev. Lett. **84**, 5824 (2000).

[3] D. C. Ralph, C. T. Black, and M. Tinkham, Phys. Rev. Lett. **74**, 3241 (1995); D. H. Cobden, M. Bockrath, P. L. McEuen, A. G. Rinzler, and R. E. Smalley, *ibid.* **81**, 681 (1998).

[4] M. Ciorga, A. S. Sachrajda, P. Hawrylak, C. Gould, P. Zawadzki, S. Jullian, Y. Feng, and Z. Wasilewski, Phys. Rev. B **61**, R16 315 (2000).

[5] R. C. Ashoori, J. A. Lebens, N. P. Bigelow, and R. H. Silsbee, Phys. Rev. B **48**, 4616 (1993).

[6] S. Tarucha, D. G. Austing, T. Honda, R. J. Van der Hage, and L. P. Kouwenhoven, Phys. Rev. Lett. **77**, 3613 (1996).

[7] D. Weinmann, W. Häusler, and B. Kramer, Phys. Rev. Lett. **74**, 984 (1995).

[8] E. Leobandung, L. Guo, Y. Wang, and S. Y. Chou, Appl. Phys. Lett. **67**, 938 (1995).

[9] L. P. Rokhinson, L. J. Guo, S. Y. Chou, and D. C. Tsui, Appl. Phys. Lett. **76**, 1591 (2000).

[10] P. L. McEuen, E. B. Foxman, Jari Kinaret, U. Meirav, M. A. Kastner, Ned S. Wingreen, and S. J. Wind, Phys. Rev. B **45**, 11 419 (1992).

[11] T. Schmidt, M. Tewordt, R. H. Blick, R. J. Haug, D. Pfannkuche, K. V. Klitzing, A. Förster, and H. Lüth, Phys. Rev. B **51**, 5570 (1995).

[12] W. G. Van der Wiel, T. H. Oosterkamp, J. W. Janssen, L. P. Kouwenhoven, D. G. Austing, T. Honda, and S. Tarucha, Physica B **256-258**, 173 (1998).

[13] T. Ando, A. B. Fowler, and F. Stern, Rev. Mod. Phys. **54**, 437 (1982).